

# VISION BASED 3D TRACKING CONTROL OF UAV

**Jahanzeb T. Khan**  
 \*University of Toronto

**Keywords:** *Vision-based Control, IBVS Control, UAV Control*

## Abstract

*This paper presents two image-based controllers designed to track a target moving at constant velocity. Dynamical model of VTOL type UAV is manipulated to facilitate the control design. The first controller is designed for known target velocity while the second controller is designed for unknown target velocity. The work is motivated by the technique of spherical-projection used to control UAV motion in 3D using only monocular vision. In both cases, the control strategy relies on designing of driving force for the translational dynamics, from which the desired orientation and thrust are extracted. Thereafter, an inner high gain feedback loop is used to generate the control torque guaranteeing the convergence of the actual attitude to the desired one.*

## 1 Introduction

Unmanned aircraft or Unmanned Aerial Vehicles (UAV) are an area of significant research activity these days. Lack of human pilot paves the way for advanced and more sophisticated control algorithms that should just not control each and every single aspect of flight dynamics but also accomplish the desired task at the same time. Visual servoing is one such way of controlling the attitude and position of aircraft by using camera as a sensor. Visual servoing has evolved into two major types over the years: Image-Based Visual Servo (**IBVS**) or Position-Based Visual Servo (**PBVS**). In position-based control, the extracted features are used along with the geometric model of the target to determine the pose of the target with respect to the camera. Image-based

approach uses the same procedure but instead of reconstructing the target position, control design is performed directly on the image features.

Generally in IBVS schemes, the depth of each feature of interest appears in the coefficients of Jacobian matrix related to the translational motion [1]. The estimation of this unknown depth is the most daunting problem of the IBVS approach due to the fact that the depth coordinate is lost when a 3D environment is projected on a 2D image surface. Various approaches have been proposed in the literature to estimate the unknown depth; these include: estimation via partial pose estimation, adaptive control, and estimation of image Jacobian using quasi-Newton techniques. Two newer, yet somewhat similar techniques have also been developed recently that rely on using a different coordinate system than Cartesian coordinates. The first one was proposed in [2] in which cylindrical coordinate system was used to control the motion of robot manipulator in 3D without knowing the depth. The other approach was proposed in [3], in which they used spherical projection to accurately control the position of UAV in three dimensions. The latter team has published several works related to IBVS control of UAVs, such as [3], [7], [8], and more. By generating a virtual 3D image surface from 2D data obtained from the image, it is possible to obtain a sense of unknown depth which can therefore be used to control the motion of UAV in 3D.

In all the works mentioned above (i.e. [3], [7], [8]), the common assumption is that the target is stationary. Some potential applications of vision-based control of autonomous helicopter

include crime-fighting or cinematography applications in which the target would most likely be moving. With the aim to develop 3D-target-features-tracking controller using only one camera, the technique of spherical-projection is borrowed from the above mentioned works and extended (to obtain error dynamics equation) for the work documented in this paper. The dynamical model of the aircraft is manipulated to facilitate the control design. Two IBVS controllers are then developed to track desired features of a moving target. The first IBVS controller design is based on the assumption that the target velocity is known, while the second one deals with unknown target velocity. The control strategy (in both cases) relies on the design of driving force for the translational dynamics, from which the desired orientation and thrust are extracted. Thereafter, an inner high gain feedback loop is used to generate the control torque guaranteeing the convergence of the actual attitude to the desired one.

This paper is organized as follows: Section 2 presents modification of dynamic model to facilitate the control design. Section 3 briefly talks about the extension to error dynamics modeling. Section 4 presents the IBVS control design to track a moving target. Simulation results are presented in Section 5 and concluding remarks are given in Section 6.

## 2 Dynamic Model Manipulation

Suppose  $I = [\hat{x}_i, \hat{y}_i, \hat{z}_i]^T$  denotes a right-hand inertial frame such that  $\hat{z}_i$  is pointing downwards into the earth. Let  $\mathcal{B}$  denote the right-hand body fixed frame given by  $\mathcal{B} = [\hat{x}, \hat{y}, \hat{z}]^T$ , the positive  $\hat{z}$  direction points downwards. It should be noted that the position of the camera, given by  $\xi = [x, y, z]^T \in I$  is measured at the center of camera instead of center of mass of the vehicle. The description of the other symbols is as follows:

- $R$ : Rotation matrix of frame I w.r.t. frame  $\mathcal{B}$ .
- $V$ : Velocity of the aircraft in  $\mathcal{B}$
- $m$ : Mass of the aircraft.
- $\tau_a$ : Torque (Control input).
- $F_d$ : External disturbance force.

$\Omega$ : Angular velocity of the aircraft expressed in  $\mathcal{B}$ .

$\varepsilon$ : Distance from the center of  $\mathcal{B}$  to the point where the disturbance forces are applied.

$l$ : Horizontal distance from the  $\hat{z}$  axis to the center of the aileron.

$I_b$ : Inertia matrix in  $\mathcal{B}$ .

For a typical aircraft evolving in air, its motion in the body-fixed frame  $\mathcal{B}$  is given by:

$$\dot{\xi} = R^T V \quad (1)$$

$$\dot{V} = -S(\Omega)V + \mu - S\left(\frac{\hat{z}}{ml}\right)\tau_a + \frac{1}{m}F_d \quad (2)$$

$$\dot{R} = -S(\Omega)R \quad (3)$$

$$I_b \dot{\Omega} = -S(\Omega)I_b \Omega + \varepsilon S(\hat{z})F_d + \tau_a \quad (4)$$

where,  $\mu$  denotes the forces acting on the system and is given by the expression  $\mu = gR\hat{z} - \frac{T}{m}\hat{z}$ . The notation  $S(\Omega)$  denotes the skew-symmetric matrix of  $\Omega$  such that  $S(\Omega)V = \Omega \times V$ .

In the dynamical model given above in Eq. (1) - Eq. (4), the control input  $\tau_a$  appears in both the translational dynamics as well as in the rotational dynamics equations. The appearance of control input in both expressions make the UAV control problem more challenging. To overcome this problem, a simple technique of change of coordinates was introduced by Olfati-Saber in his work [4]. By extending the work from 2D, as proposed in the original work [4], to 3D as done in [5], the control input can easily be removed from translational dynamics relations. Consider the following change of variables,

$$\bar{V} = V + S\left(\frac{\hat{z}}{ml}\right)I_b \Omega \quad (5)$$

Using the identity

$$\left( S(\Omega)S\left(\frac{\hat{z}}{ml}\right) - S\left(\frac{\hat{z}}{ml}\right)S(\Omega) \right) I_b \Omega = \frac{1}{ml}S(I_b \Omega)S(\Omega)\hat{z} \quad (6)$$

the translational dynamics can be rewritten as

$$\dot{\xi} = R^T \left( \bar{V} - S\left(\frac{\hat{z}}{ml}\right)I_b \Omega \right) \quad (7)$$

$$\dot{\bar{V}} = -S(\Omega)\bar{V} + \mu - \frac{1}{ml}S(I_b\Omega)S(\Omega)\hat{z} + f(\varepsilon, m, l, F_d) \quad (8)$$

where  $f(\varepsilon, m, l, F_d) = \frac{1}{ml}(II_{3 \times 3} + \varepsilon S^2(\hat{z}))F_d = [\frac{(l-\varepsilon)F_{d1}}{ml}, \frac{(l-\varepsilon)F_{d2}}{ml}, \frac{F_{d3}}{ml}]^T$ , with  $F_d = [F_{d1}, F_{d2}, F_{d3}]^T$ . By using the fact that  $I_b = \text{diag}[I_1, I_1, I_2]$ , and letting  $\bar{\xi} = \xi - \frac{I_1}{ml}R^T\hat{z}$ , it can be shown that

$$\bar{v} = v - \frac{I_1}{ml}R^T S(\Omega)\hat{z} \quad (9)$$

where  $v = \dot{\xi}$  and  $\bar{v} = \dot{\bar{\xi}}$ . The velocity  $\bar{v}$  can be expressed in the body-fixed frame as

$$\begin{aligned} R\bar{v} &= Rv - \frac{I_1}{ml}RR^T S(\Omega)\hat{z} \\ \bar{V} &= V + \frac{I_1}{ml}S(\hat{z})\Omega \\ &= V + S(\frac{\hat{z}}{ml})I_b\Omega \end{aligned}$$

The symbols  $v$  and  $\bar{v}$  have usual meanings as above but are used to express the respective velocities in  $I$ . Let  $\bar{\xi}_b = R\bar{\xi}$  denote the position of the aircraft in the body-fixed frame. Hence the full dynamical model of the system is given by the following four equations.

$$\dot{\bar{\xi}}_b = -S(\Omega)\bar{\xi}_b + \bar{V} \quad (10)$$

$$\dot{\bar{V}} = -S(\Omega)\bar{V} + \mu - \frac{1}{ml}S(I_b\Omega)S(\Omega)\hat{z} + f(\varepsilon, m, l, F_d) \quad (11)$$

$$\dot{R} = -S(\Omega)R \quad (12)$$

$$I_b\dot{\Omega} = -S(\Omega)I_b\Omega + \varepsilon S(\hat{z})F_d + \tau_a \quad (13)$$

### 3 Error Dynamics Modeling

The error dynamics are modeled in [3] for a stationary target (i.e.  $V_T = 0$ ). By following the original work, the tracking error dynamics can be derived assuming that the desired image features have a fixed location on the image-plane. The full tracking error dynamics of the image error  $\delta_p$  can be written as

$$\dot{\delta}_p = -S(\Omega)\delta_p + Q(V_T - \bar{V}) \quad (14)$$

$$\dot{\bar{V}} = -S(\Omega)\bar{V} + \mu - \frac{1}{ml}S(I_b\Omega)S(\Omega)\hat{z} + f(\varepsilon, m, l, F_d) \quad (15)$$

$$\dot{R} = -S(\Omega)R \quad (16)$$

$$I_b\dot{\Omega} = -S(\Omega)I_b\Omega + \varepsilon S(\hat{z})F_d + \tau_a \quad (17)$$

The above error dynamics will be used in the next section to derive the control law.

## 4 Control Design

In this section, two IBVS controllers are designed to track a moving target. It is assumed that the UAV is hovering in air at some distance away from the target and the target is moving in a small neighborhood. In designing the control laws, it is assumed that all target points are visible by the camera at all times.

### 4.1 IBVS Control Design 1

The control law derived in this section assumes that the target is moving at a constant known velocity  $V_T$  in  $\mathcal{B}$ . Pick  $\bar{V}$  as virtual control and set it as

$$\bar{V} = V_T + k_1\delta_p \quad (18)$$

where  $k_1$  is a scalar gain. For a Lyapunov function candidate of the form  $\frac{1}{2}\delta_p^T\delta_p$ , using the virtual control of  $\bar{V}$  as mentioned above would result in the derivative of Lyapunov function to be negative definite in  $\delta_p$  and would therefore guarantee the exponential convergence of the error  $\delta_p$ .

The velocity  $\bar{V}$  can not be directly assigned in a physical system due to the fact that  $\tau_a$  is the control input. To continue the back-stepping procedure, let  $\delta_v$ , the **velocity error**, be the error between the camera velocity and the target velocity plus an additional term  $\delta_p$ , i.e.

$$\delta_v = \bar{V} - k_1\delta_p - V_T \quad (19)$$

The dynamics of the error  $\delta_v$  in view of Eq. 14 and Eq. 15 will be given

$$\begin{aligned} \dot{\delta}_v &= \mu - \frac{1}{ml}S(I_b\Omega)S(\Omega)\hat{z} + f(\varepsilon, m, l, F_d) + k_1Q\delta_v \\ &\quad - k_1Q(-k_1\delta_p) - S(\Omega)V_T - \dot{V}_T \end{aligned}$$

Let,

$$\mathcal{L} = \frac{1}{2}\delta_p^T \delta_p + \frac{1}{2}\delta_v^T \delta_v + \frac{1}{2\Gamma}\tilde{F}^T \tilde{F} \quad (20)$$

be a candidate Lyapunov function where  $\tilde{F} = F_d - \hat{F}_d$  and  $\Gamma$  is a positive scalar gain.

**THEOREM 4.1** By picking the control effort  $\mu$  as,

$$\begin{aligned} \mu = & \frac{1}{ml}S(I_b\Omega)S(\Omega)\hat{z} - \frac{1}{ml}(II_{3\times 3} + \varepsilon S^2(\hat{z}))\hat{F}_d \\ & + S(\Omega)V_T - k_2\delta_v + \dot{V}_T \end{aligned} \quad (21)$$

where  $k_2$  is a scalar gain satisfying the condition  $k_2 > k_1\lambda_{\max}(Q)$  and setting the derivative of the estimation of unknown disturbance force as

$$\dot{\hat{F}}_d = \frac{\Gamma}{ml}(II_{3\times 3} + \varepsilon S^2(\hat{z}))\delta_v$$

the errors  $\delta_p$  and  $\delta_v$  can be minimized.

**PROOF:** The time derivative of the Lyapunov function is given by

$$\begin{aligned} \dot{\mathcal{L}} = & \delta_p^T (Q(-k_1\delta_p) - Q\delta_v) + \delta_v^T (\mu - \\ & \frac{1}{ml}S(I_b\Omega)S(\Omega)\hat{z} + \frac{1}{m}(II_{3\times 3} + \varepsilon S^2(\hat{z}))F_d + k_1Q\delta_v \\ & (-S(\Omega)V_T - k_1Q(-k_1\delta_p) - \dot{V}_T) - \frac{1}{\Gamma}\tilde{F}^T \dot{\hat{F}}_d \end{aligned}$$

By substituting the expressions of  $\dot{\hat{F}}_d$  and  $\mu$ , the derivative of Lyapunov candidate function can be written in the simplified form as

$$\begin{aligned} \dot{\mathcal{L}} = & -k_1\delta_p^T Q\delta_p - (1 - k_1)\delta_p^T Q\delta_v - \delta_v^T \\ & (k_2I_{3\times 3} - k_1Q)\delta_v \end{aligned}$$

In order to guarantee convergence of the errors  $\delta_p$  and  $\delta_v$ , the Young's inequality can be applied to obtain conditions on gains  $k_1$  and  $k_2$ . Using Young's inequality, one obtains the condition

$$\begin{aligned} \dot{\mathcal{L}} \leq & -[k_1\lambda_{\min}(Q) - \varepsilon_1(1 + k_1)]\|\delta_p\|^2 - \\ & [k_2 - k_1\lambda_{\max}(Q) - \frac{k_1 + 1}{4\varepsilon_1}\lambda_{\max}^2(Q)]\|\delta_v\|^2 \end{aligned}$$

From the above expressions, it can be concluded that the following two conditions must be satisfied

$$k_1\lambda_{\min}(Q) - \varepsilon_1(1 + k_1) > 0$$

$$k_2 - k_1\lambda_{\max}(Q) - \frac{k_1 + 1}{4\varepsilon_1}\lambda_{\max}^2(Q) > 0$$

for any  $\varepsilon_1 > 0$ , where  $\varepsilon_1$  is a Young's equation constant. This result guarantees the global boundedness of  $\delta_p$  and  $\delta_v$  as well as their convergence to zero when time goes to infinity.

## 4.2 IBVS Control Design 2

In this section, an IBVS control law capable of following a moving target with an unknown velocity will be derived. The adaptive term  $\hat{V}_T$  will estimate the unknown constant velocity  $V_T$  and the error  $\tilde{V}$  will be used to measure the difference between  $\hat{V}_T$  and  $V_T$ . Once again, pick  $\bar{V}$  as virtual control and set it as

$$\bar{V} = \hat{V}_T + \bar{k}\delta_p \quad (22)$$

and let  $\tilde{V}$  be equal to

$$\tilde{V} = \hat{V}_T - V_T - k\delta_p \quad (23)$$

where  $\bar{k}$  and  $k$  are scalar gains greater than zero ( $\bar{k} > 0$ ,  $k > 0$ ). The following development using  $\mathcal{L}_1$  as a Lyapunov function candidate shows why the errors  $\delta_p$  and  $\tilde{V}$  can be minimized but not guaranteed to converge to zero. The backstepping procedure to complete the control design is continued from there on. Let,

$$\mathcal{L}_1 = \frac{1}{2}\delta_p^T \delta_p + \frac{1}{2}\tilde{V}^T \tilde{V} \quad (24)$$

be a candidate Lyapunov function. Using the dynamics of  $\delta_p$  from Eq. 14 and  $\tilde{V}$  from Eq. 23, the derivative of  $\mathcal{L}_1$  is given by

$$\begin{aligned} \dot{\mathcal{L}}_1 = & \delta_p^T (-S(\Omega)\delta_p + Q(V_T - \bar{V})) + \tilde{V}^T \left( \dot{\hat{V}}_T \right. \\ & \left. + kS(\Omega)\delta_p - kQ(V_T - \bar{V}) \right) \end{aligned}$$

Set  $\dot{\hat{V}}_T$  as follows:

$$\dot{\hat{V}}_T = -kS(\Omega)\delta_p - \beta(\hat{V}_T - k\delta_p) \quad (25)$$

with  $\beta$  being a scalar gain greater than zero ( $\beta > 0$ ). The derivative of the Lyapunov function candidate  $\dot{\mathcal{L}}_1$  will therefore be given by

$$\dot{\mathcal{L}}_1 = \delta_p^T Q(V_T - \hat{V}_T - \bar{k}\delta_p) + \tilde{V}^T (-\beta(\tilde{V} + V_T))$$

$$-kQ(V_T - \hat{V}_T - \bar{k}\delta_p))$$

which can be simplified as

$$\begin{aligned} \dot{L}_1 = & -(k + \bar{k})\delta_p^T Q \delta_p - \tilde{V}^T (\beta I_{3 \times 3} - kQ) \tilde{V} \\ & - \tilde{V}^T (Q - (k + \bar{k})kQ) \delta_p - \tilde{V}^T \beta V_T \end{aligned}$$

Due to the structure of the derivative Lyapunov function candidate (i.e. square terms in  $\delta_p$  and  $\tilde{V}$ , cross term of  $\delta_p$  and  $\tilde{V}$ , and an extra  $V_T$  term), the exponential convergence of  $\delta_p$  to zero can not be guaranteed because of the ‘‘disturbance’’ term  $\tilde{V}^T \beta V_T$ . In order to guarantee the boundedness of the error  $\delta_p$ , the eigenvalues of term  $[\beta I_{3 \times 3} - kQ]$  should be greater than zero.

The virtual control of  $\bar{V}$  can not be directly assigned and backstepping procedure needs to be continued. Let  $\delta_v$  denote the difference between the camera velocity and the target velocity, plus an additional term in  $\delta_p$ . Therefore,  $\delta_v$  is given by

$$\delta_v = \bar{V} - \hat{V}_T - \bar{k}\delta_p \quad (26)$$

the time derivative of which is

$$\begin{aligned} \dot{\delta}_v = & \dot{\bar{V}} - \dot{\hat{V}}_T - \bar{k}\dot{\delta}_1 \\ = & -S(\Omega)\bar{V} + \mu - \frac{1}{ml}S(I_b\Omega)S(\Omega)\hat{z} + \\ & f(\epsilon, m, l, F_d) - (-kS(\Omega)\delta_p - \beta(\hat{V}_T - k\delta_p)) \\ & - \bar{k}(-S(\Omega)\delta_p + Q(V_T - \bar{V}) - Q\delta_v) \quad (27) \end{aligned}$$

Let,

$$\mathcal{L} = \frac{1}{2}\delta_p^T \delta_p + \frac{1}{2}\delta_v^T \delta_v + \frac{1}{2}\tilde{V}^T \tilde{V} + \frac{1}{2\Gamma}\tilde{F}^T \tilde{F} \quad (28)$$

be a Lyapunov candidate function with  $\tilde{F} = F_d - \hat{F}_d$  and  $\Gamma$  is a positive scalar gain as before.

**THEOREM 4.2** By picking  $\hat{V}_T$  as in Eq. 25, setting the control effort  $\mu$  as

$$\begin{aligned} \mu = & S(\Omega)\bar{V} + \frac{1}{ml}S(I_b\Omega)S(\Omega)\hat{z} - (k + \bar{k})S(\Omega)\delta_p \\ & - \beta(\hat{V}_T - k\delta_p) - \frac{1}{ml}(I_{3 \times 3} + \epsilon S^2 \hat{z})\hat{F}_d \\ & - k_2\delta_v \quad (29) \end{aligned}$$

and the derivative of  $\hat{F}_d$  as in previous controller, i.e.

$$\dot{\hat{F}}_d = \frac{\Gamma}{ml}(I_{3 \times 3} + \epsilon S^2(\hat{z}))\delta_v$$

the errors  $\delta_p$ ,  $\delta_v$ , and  $\tilde{V}$  can be minimized.  $k_2$  is a scalar gain greater than the maximum eigenvalue of the matrix  $Q$  (i.e.  $k_2 > \lambda_{\max}(Q)$ ).

**PROOF** The time derivative of this Lyapunov candidate function, in view of Eq. 14, Eq. 23, Eq. 25, and Eq. 27, is

$$\begin{aligned} \dot{L} = & \delta_p^T (Q(V_T - \hat{V}_T - \bar{k}\delta_p) - Q\delta_v) + \tilde{V}^T (-kS(\Omega)\delta_p \\ & - \beta(\hat{V}_T - k\delta_p) - k(-S(\Omega)\delta_p + Q(V_T - \hat{V}_T - \bar{k}\delta_p) \\ & - Q\delta_v) + \delta_v^T \left( -S(\Omega)\bar{V} + \mu - \frac{1}{ml}S(I_b\Omega)S(\Omega)\hat{z} + \right. \\ & f(\epsilon, m, l, F_d) + kS(\Omega)\delta_p + \beta(\hat{V}_T - k\delta_p) + \bar{k}S(\Omega)\delta_p \\ & \left. + \bar{k}Q\delta_v - \bar{k}Q(V_T - \hat{V}_T - \bar{k}\delta_p) \right) - \tilde{F}^T \dot{\hat{F}}_d \end{aligned}$$

By plugging in the expressions of  $\mu$  and  $\dot{\hat{F}}_d$  one can get simplified time derivative of Lyapunov function candidate as

$$\begin{aligned} \dot{L} = & -(k + \bar{k})\delta_p^T Q \delta_p - \delta_v^T (-\bar{k}Q + k_2 I_{3 \times 3}) \delta_v - \\ & \tilde{V}^T (\beta I_{3 \times 3} - kQ) \tilde{V} - (1 - \bar{k}(k + \bar{k})) \delta_p^T Q \delta_v - \tilde{V}^T (Q \\ & - k(k + \bar{k})Q - kI_{3 \times 3}) \delta_p + (k + \bar{k})\delta_v^T Q \tilde{V} - \beta \tilde{V}^T V_T \end{aligned}$$

Once again apply Young’s inequality to obtain conditions on gains to guarantee convergence.

$$\dot{L} \leq - \left( (k + \bar{k})\lambda_{\min}(Q) - (1 + \bar{k}(k + \bar{k}))\epsilon_1 - \frac{1}{4\epsilon_3} \right.$$

$$\begin{aligned} & \left. \|\Delta\|^2 \right) \|\delta_p\|^2 - (k_2 - \bar{k}\lambda_{\max}(Q) - (\bar{k} + k)\epsilon_2 - \\ & \frac{1 + \bar{k}(k + \bar{k})}{4\epsilon_1} \lambda_{\max}^2(Q)) \|\delta_v\|^2 - (\beta - k\lambda_{\max}(Q) - \\ & \frac{\bar{k} + k}{4\epsilon_2} \lambda_{\max}^2(Q) - \epsilon_3 - \beta\epsilon_4) \|\tilde{V}\|^2 + \frac{\beta}{4\epsilon_4} \|V_T\|^2 \end{aligned}$$

where,  $\Delta = Q - k(k + \bar{k})Q - kI_{3 \times 3}$ . Assume that,

$$(k + \bar{k})\lambda_{\min}(Q) - (1 + \bar{k}(k + \bar{k}))\epsilon_1 - \frac{1}{4\epsilon_3} \|\Delta\|^2 = \alpha_1$$

$$k_2 - \bar{k}\lambda_{\max}(Q) - (\bar{k} + k)\epsilon_2 - \frac{1 + \bar{k}(k + \bar{k})}{4\epsilon_1} \lambda_{\max}^2(Q)$$

$$= \alpha_2$$

$$\beta - k\lambda_{\max}(Q) - \frac{\bar{k} + k}{4\epsilon_2} \lambda_{\max}^2(Q) - \epsilon_3 - \beta\epsilon_4 = \alpha_3$$

Using the above simplifications, the time derivative of Lyapunov candidate function can be written as

$$\dot{L} = -\alpha_1 \|\delta_p\|^2 - \alpha_2 \|\delta_v\|^2 - \alpha_3 \|\tilde{V}\|^2 + \frac{\beta}{4\epsilon_4} \|V_T\|^2 \quad (30)$$

Therefore, for some positive Young's equation constants  $\epsilon_1$ ,  $\epsilon_2$ ,  $\epsilon_3$ , and  $\epsilon_4$ , the following three conditions must be satisfied to guarantee the boundedness of the errors  $\delta_p$ ,  $\delta_v$ , and  $\tilde{V}$  and their convergence to domain

$$D = \left( \delta_p, \delta_v, \tilde{V} / \alpha_1 \|\delta_p\|^2 + \alpha_2 \|\delta_v\|^2 + \alpha_3 \|\tilde{V}\|^2 \leq \frac{\beta}{4\epsilon_4} \|V_T\|^2 \right), \text{ and}$$

$$\alpha_1 > 0, \alpha_2 > 0, \alpha_3 > 0$$

### 4.3 Quaternion Extraction

In the previous section, the force,  $\mu$ , required to move the airborne vehicle closer to the target was derived. In order to apply the desired forces on the system, the attitude of the aircraft must be changed through changing the thrust and the torque. The quantity  $\mu$  contains information about the desired thrust as well as the attitude and extracting this desired information properly is achieved through quaternion extraction. A secondary negative feedback controller is then required to compare and minimize the difference between the desired angular velocity and the instantaneous angular velocity. A simple high-gain negative feedback loop is introduced in the control scheme inside the main control loop for this purpose as shown in Fig. 1. The force  $\mu$  is given by

$$\mu \equiv gR\hat{z} - \frac{T}{m}\hat{z} \quad (31)$$

Substituting the relationship between rotation matrix R and quaternion Q given by

$$R = I_{3 \times 3} + 2S(q)^2 - 2q_0S(q) \quad (32)$$

into Eq. 31, it can be shown that the relationship between  $\mu$  and quaternion Q is

$$\mu = g \begin{pmatrix} 2q_1q_3 - 2q_0q_2 \\ 2q_2q_3 + 2q_0q_1 \\ -\frac{T}{mg} + 1 - 2(q_1^2 + q_2^2) \end{pmatrix}$$

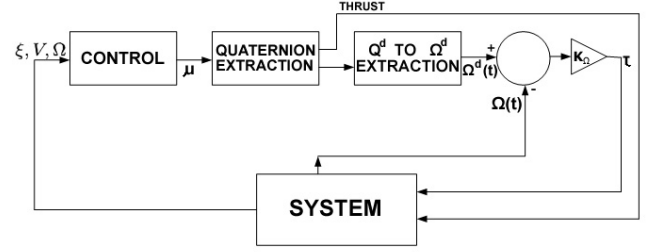


Fig. 1 Block diagram

Assuming that  $q_3 = 0$  for simplification and setting thrust as

$$T := mg(\alpha q_0^2 + 1 - 2(q_1^2 + q_2^2)) \quad (33)$$

with  $\alpha$  being a variable the value of which will be determined later. This leads to

$$\begin{pmatrix} \mu_1 \\ \mu_2 \\ \mu_3 \end{pmatrix} = g \begin{pmatrix} -2q_0q_2 \\ 2q_0q_1 \\ -\alpha q_0^2 \end{pmatrix}$$

Let,

$$\eta_1 = \mu_1^2 + \mu_2^2 = 4g^2q_0^2(q_1^2 + q_2^2) = 4g^2q_0^2(1 - q_0^2) \quad (34)$$

The solution of above equation can be found using the quadratic formula and is given by

$$q_0^2 = \frac{g + \sqrt{g^2 - \eta_1}}{2g} = \frac{\eta_2}{2g} \quad (35)$$

with  $n_1 \leq g^2$ . It can be easily verified that the range of  $q_0^2$  is between 0 and 1. The other solution of  $q_0^2$  is ignored because it will yield  $q_0 = 0$  for  $\eta_1 = 0$ . If the conditions  $|\mu_1| < 2g$  and  $|\mu_2| < 2g$  are imposed, then the solution of  $q_1$  and  $q_2$  are

$$q_1 = \frac{\mu_2}{2gq_0}$$

$$q_2 = \frac{\mu_1}{2gq_0}$$

Now that all the components of quaternion have been found, the value of  $\alpha$  can be determined to guarantee that the thrust 'T' is always positive. By choosing

$$\alpha = -\frac{\mu_3}{gq_0^2} \quad (36)$$

the condition on  $\mu_3$  can be derived to keep the thrust positive all the time. Substituting the expressions of  $q_0, q_1, q_2$ , and  $\alpha$  in Eq. 33, one gets

$$-\frac{\mu_3}{g} + 1 - 2 \left( \frac{2g\mu_2^2}{4g^2\eta_2} + \frac{2g\mu_1^2}{4g^2\eta_2} \right) > 0$$

$$\mu_3 < g - \frac{\eta_1}{\eta_2}$$

Therefore, by calculating the components of quaternion using the formulae,

$$q_0 = \sqrt{\frac{\eta_2}{2g}} \quad (37)$$

$$q_1 = \frac{\mu_2}{\sqrt{2g\eta_2}} \quad (38)$$

$$q_2 = -\frac{\mu_1}{\sqrt{2g\eta_2}} \quad (39)$$

$$q_3 = 0 \quad (40)$$

where,

$$\eta_1 = \mu_1^2 + \mu_2^2 \quad (41)$$

$$\eta_2 = g + \sqrt{g^2 - \eta_1} \quad (42)$$

$$(43)$$

and satisfying the following two conditions,

$$\mu_1^2 + \mu_2^2 \leq g^2 \quad (44)$$

$$\mu_3 < g - \frac{\mu_1^2 + \mu_2^2}{g + \sqrt{g^2 - \mu_1^2 - \mu_2^2}} \quad (45)$$

it can be guaranteed that a feasible solution exists. By satisfying the above conditions, the desired thrust can be extracted along with the four elements of quaternion which can then be used for obtaining the desired angular velocity  $\Omega^d$  as shown in [6]. The control input  $\tau_a$  is generated using a high gain feedback as follows:

$$\tau_a = K_\Omega \left( \Omega^d - \Omega \right) \quad (46)$$

The thrust extracted above along with the control torque  $\tau_a$  are then fed back into the system's dynamical model (Eq. 11 and Eq. 13) to change the position of the aircraft.

## 5 Simulation Results

The simulation results for both controllers, 'Controller 1' and 'Controller 2' are presented in this section. The inertia matrix,  $I_b$ , used is  $\text{diag}[0.5, 0.5, 0.25]N.m^2$ , the initial conditions of the rotation matrix are  $I_{3 \times 3}$ . The mass of the system is 4.313kg while the vertical lever arm  $l$  is 0.1778m.

### 5.1 CONTROLLER 1

In the simulations of the first control law, it is assumed that the target velocity is known. A disturbance force of  $F_d = -[1, 1, 0]^T N$  is applied at a distance of 0.1m above the center of the lens of the camera. The initial position of the camera is  $\xi = [-1.3, 2, -4]^T m$  in  $\mathcal{B}$  and the desired image features vector is  $\sum p_i^* = [0, 0, 1.993]^T$  corresponding to a location of  $[0, 0.75, -3]^T m$ . There are two targets points, separated by a distance of 0.5m, moving with a constant velocity of  $\pm[0.025, 0, 0]^T m/s$  in a neighborhood of 2.5m on the floor. The first target point starts its journey at  $[0, 0.5, 0]^T m$ , travels linearly a distance of 2.5m in the x-direction, and then travels backward to its origin in the same fashion. The second target point starts its journey at  $[0, 1, 0]^T$  and moves in the same way as the first target point in the x-direction. The values of the gains and other constants used are as follows:

$$k_1 = 15, k_2 = 0.4, \Gamma = 0.1, k_\Omega = 200$$

The control effort of Eq. 21 is applied to the aircraft and the simulation results are shown in Fig. 2 - Fig. 4.

It can be noticed that the error  $\delta_p$  does not converge exactly to zero which is due to the trade-off between the control torque and the error  $\delta_p$ . In order to obtain convergence to zero of the error  $\delta_p$ , much greater values of control torque,  $\tau_a$ , are required especially when the target switches its velocity. The results shown above are a good balance of the required control torque and the error  $\delta_p$ .

It can be seen in the above simulation results that there are repeated oscillations at 120 seconds

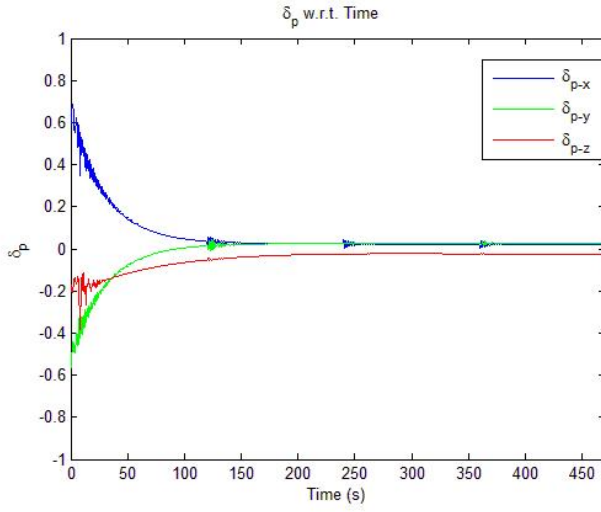


**Fig. 2** Error between desired and instantaneous image features,  $\delta_p$ , w.r.t. time.

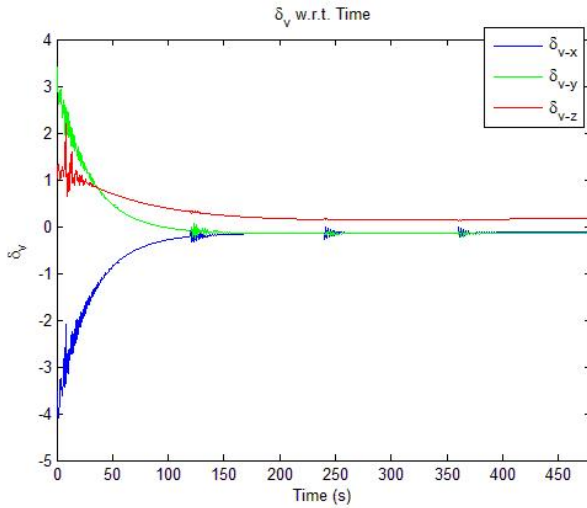


**Fig. 3** The x,y,z components of velocity error,  $\delta_v$ , with known  $V_T$ .

Evolution of Aircraft Position

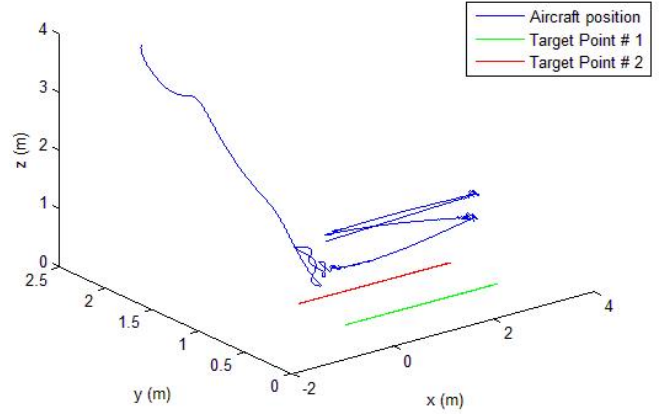


**Fig. 4** Evolution of camera position w.r.t. time.

interval in  $\delta_p$ ,  $\delta_v$ , and thrust along with spikes in the control input  $\tau_a$ . This occurs when the target changes its direction instantaneously and the UAV has to move in opposite direction all of a sudden which requires high torque momentarily.

## 5.2 CONTROLLER 2

The control effort expressed in Eq. 29 is applied to the aircraft. The initial position of the camera is  $-[3, 3, 9]m$  in  $\mathcal{B}$ , while the desired image features vector  $\Sigma p_d^* = [0, 0, 1.985]^T$  corresponding to a location of  $[0, -1, -8]^T m$ . The initial position of the first target point is  $[0, 0, 0]^T m$  while the initial position of the second target point is  $[0, -2, 0]^T$ . Both target points are moving linearly at a constant velocity of  $-[0.05, 0.05, 0]^T m/s$  in  $\mathcal{B}$ . A disturbance force,  $F_d = -[1, 1, 0]N$  was applied at a distance of 0.1m below the center of lens of the camera. The values of the other gains are as follows:  $\bar{k} = 1.5$ ,  $\beta = 0.75$ ,  $k = 0.01$ ,  $k_2 = 50$ ,  $\Gamma = 0.01$ ,  $K_\Omega = 20000$

The simulation results are shown in Fig. 5 - Fig. 9:

## 6 Conclusion

In this paper, two image-based control laws are derived to track a target moving on a plane



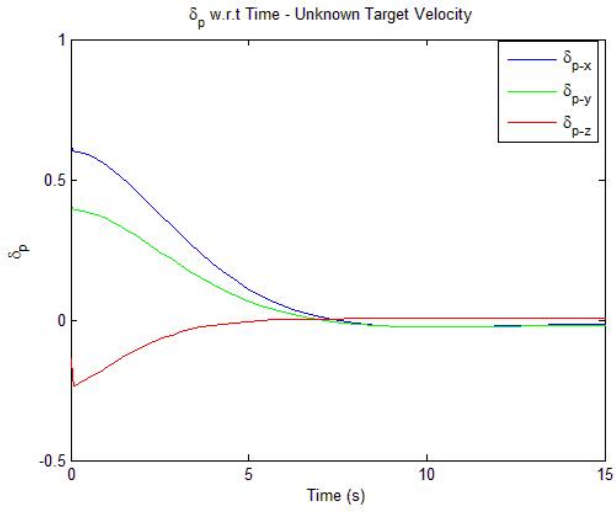


**Fig. 5** The transition of x,y,z components of  $\delta_p$  with unknown  $V_T$ .

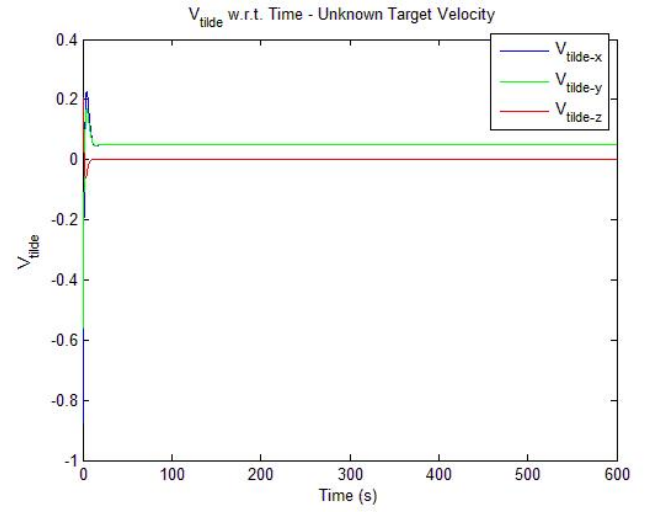


**Fig. 7** The x,y,z components of  $\tilde{V}$  with unknown  $V_T$ .

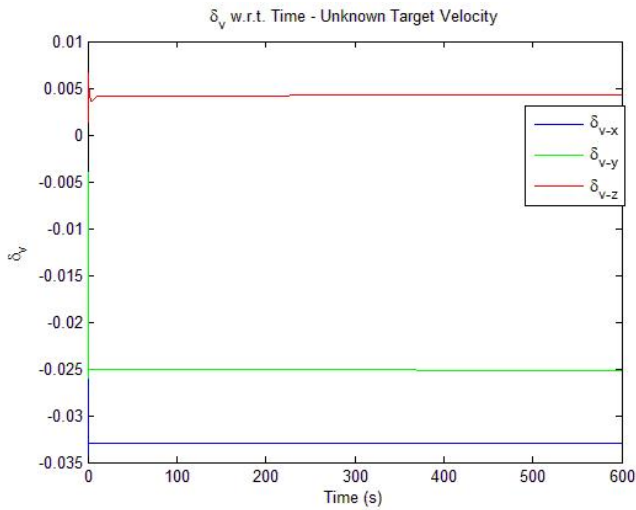


**Fig. 6** The transition of x,y,z components of  $\delta_v$  with unknown  $V_T$ .

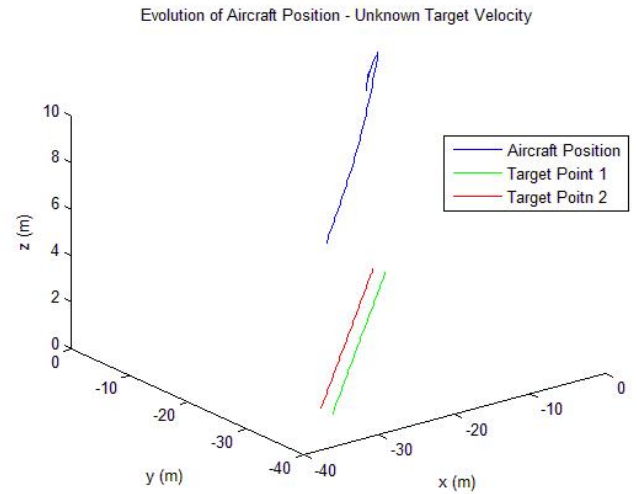


**Fig. 8** The evolution of camera position w.r.t time - unknown  $V_T$ .

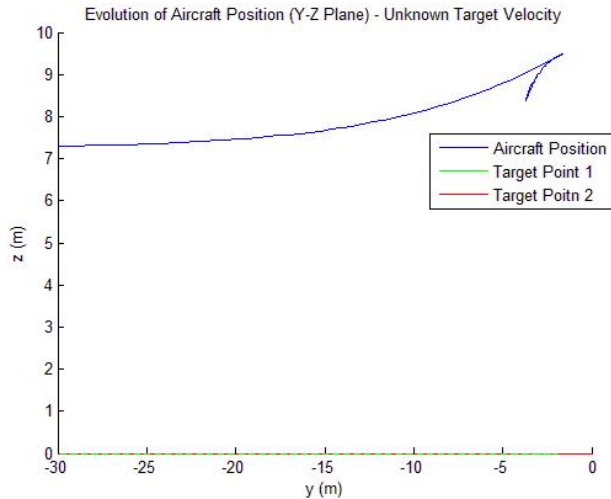


**Fig. 9** The evolution of camera position on Y-Z plane w.r.t time - unknown  $V_T$ .

surface. For known target velocity, a simple dynamic control law is sufficient while for unknown target velocity, an adaptive control law is derived to minimize the error between the desired and instantaneous image features. Even though the UAV’s motion is controlled successfully in 3D using only monocular vision, the desired height cannot be maintained due to the fact that desired features have a fixed location on image-plane. This assumption helped in simplifying the analysis but it limits the practicality of the controllers. Nevertheless, the proposed work can still be used to observe the features of a moving target. The technique of spherical projection is useful to control UAV motion w.r.t. stationary target but tends to under-perform for mobile target scenario. Simulation results show that the adaptive control law provides much smooth flight than the simple dynamic control. Future work may involve the introduction of cross-coupled terms that may not exist in theory but are always present in practical implementation.

## References

- [1] F. Chaumette, and S. Hutchinson, “Visual Servo Control, Part II: Advanced Approaches ” *IEEE Robotics and Automation Magazine*, Vol. 14, No. 1, pp. 109-118, Mar 2007.
- [2] M. Iwatsuki, and N. Okiyama, “A new formulation of visual servoing based on cylindrical coordinate system” *IEEE Transactions on Robotics and Automation*, Vol. 21, No. 2, pp. 266-273, Apr 2005.
- [3] T. Hamel, and R. Mahony, “Visual servoing of an under-actuated dynamic rigid-body system: an image-based approach” *IEEE Transactions on Robotics and Automation*, Vol. 18, No. 2, pp. 187-198, Apr 2002.
- [4] R. Olfati-Saber, “Global configuration stabilization for the VTOL Aircraft with Strong Input Coupling” *IEEE Transactions on Automatic Control*, Vol. 47 No. 11, pp. 1949 - 1952, 2002.
- [5] J. Pfimlin, P. Soueres, and T. Hamel, “Hovering flight stabilization in wind gusts for ducted fan UAV” *43rd IEEE Conference on Decision and Control*, pp. 3491 - 3496, 2004.
- [6] A. Tayebi, S. McGilvray, A. Roberts, and M. Moallem, “Attitude estimation and stabilization of a rigid body using low-cost sensors”, *In proceedings of the 46th IEEE conference on decision and control*, New Orleans, LA, USA, 2007.
- [7] N. Guenard, T. Hamel, and R. Mahony, “A Practical Visual Servo Control for an Unmanned Aerial Vehicle” *IEEE Transactions on Robotics*, Vol. 24, No. 2, pp. 331-340, Apr 2008.
- [8] B. Herisse, Francois-Xavier Russotto, Tarek Hamel, and Robert Mahony, “Hovering flight and vertical landing control of a VTOL Unmanned Aerial Vehicle using Optical Flow” *IEEE/RSJ International Conference on Intelligent Robotics and Systems*, pp. 801 -808, 2008.

## Copyright Statement

The author confirm that he holds copyright on all of the original material included in this paper. The author also confirm that they have obtained permission, from the copyright holder of any third party material included in this paper, to publish it as part of his paper. The author confirms that he gives permission, for the publication and distribution of this paper as part of the ICAS2010 proceedings or as individual off-prints from the proceedings.